ARTICLE
Traditional Medicine Research 2025;10(11):65. https://doi.org/10.53388/TMR20241216001

An integrated network pharmacological approach unveils the therapeutic mechanism of bonducellin, a homoisoflavonoid from *Caesalpinia bonducella*, against polycystic ovary syndrome

Manivannan Karthikeyan[1], Sarvesh Sabarathinam[2], Harikrishnan Mohan[3], Balasundaram Usha[1*]

[1]Medicinal Plants and PCOS Research Laboratory, Department of Genetic Engineering, SRM Institute of Science and Technology, Kattankulathur 603203, India. [2]Department of Psychiatry, Saveetha Medical College and Hospitals, Saveetha Institute of Medical and Technical Sciences, Saveetha University, Chennai 602105, India. [3]Department of Pathobiological Sciences, School of Veterinary Medicine, Louisiana State University, Baton Rouge 70803, United States.

[*]**Correspondence to:** Balasundaram Usha. Medicinal Plants and PCOS Research Laboratory, Department of Genetic Engineering, SRM Institute of Science and Technology, Kattankulathur, Tamil Nadu-603203, India. E-mail: sundaram.usha@gmail.com.

Author contributions

Karthikeyan M contributed to the conceptualization, investigation, data analysis, and original manuscript drafting. Mohan H, Karthikeyan M and Sabarathinam S performed molecular simulation and data analysis. Usha B conceptualized and designed the study, reviewed and edited the manuscript, and provided overall supervision. All authors read and approved the final manuscript.

Competing interests

The authors declare no conflicts of interest.

Acknowledgments

All authors thank the High-Performance Computing Centre, SRM Institute of Science and Technology, for providing computational facilities.

Peer review information

Traditional Medicine Research thanks Hong Li and other anonymous reviewers for their contribution to the peer review of this paper.

Abbreviations

AR, androgen receptor; BRAF, B-Raf proto-oncogene (serine/threonine-protein kinase); CYP19A1, cytochrome P450 family 19 subfamily A member 1 (aromatase); GnRH, gonadotropin-releasing hormone; HSD11B1, hydroxysteroid 11-beta dehydrogenase 1; HSD17B2, 17beta-hydroxysteroid dehydrogenase type 2; KDR, Kinase Insert Domain Receptor; KIT, Protooncogene C KIT (Tyrosine Protein Kinase); MMP9, Matrix Metalloproteinase-9; PCOS, polycystic ovary syndrome; PDB, Protein Data Bank; PIK3R1, phosphoinositide-3-kinase regulatory subunit 1; PRKACA, protein kinase cAMP-activated catalytic subunit alpha; PRKCA, protein kinase C alpha; RAF1, Raf-1 Proto-Oncogene (Serine/Threonine Kinase); ROCK1, Rho-associated protein kinase 1; STAT3, Signal Transducer and Activator for Transcription 3; PPI, Protein-Protein Interaction; LH, luteinizing hormone; FSH, follicle-stimulating hormone; GO, Gene Ontology; KEGG, Kyoto Encyclopedia of Genes and Genomics; MD, molecular dynamics; RMSD, root mean square deviation; RMSF, root mean square fluctuation; cDNA, complementary DNA; RT-PCR, reverse transcription polymerase chain reaction; TIMPs, tissue inhibitors of MMPs; CC, clomiphene citrate.

Citation

Karthikeyan M, Sabarathinam S, Mohan H, Usha B. An integrated network pharmacological approach unveils the therapeutic mechanism of bonducellin, a homoisoflavonoid from *Caesalpinia bonducella*, against polycystic ovary syndrome. *Tradit Med Res.* 2025;10(11):65. doi: 10.53388/TMR20241216001.

Executive editor: Xin-Yue Zhang.

Received: 16 December 2024; **Revised:** 27 March 2025; **Accepted:** 22 April 2025; **Available online:** 28 May 2025.

Abstract

Background: Bonducellin is one of the bioactive compounds present in *Caesalpinia bonduc* Roxb (L). It is a homoisoflavonoid recognized for its anti-cancer, anti-androgenic, and anti-estrogenic properties and could potentially treat polycystic ovary syndrome (PCOS). However, the underlying molecular mechanism remains unexplored. This study aims to elucidate the potential molecular mechanisms of bonducellin in treating PCOS and its associated symptoms through an integrated approach combining network pharmacology, molecular docking, molecular dynamics simulation, and *in vivo* validation. **Methods:** Bonducellin-associated and PCOS-related genes were intersected using VENN analysis to determine common gene targets. KEGG pathway analysis was conducted to investigate the biological pathways involving the co-targeted genes. The protein-protein interactions of the target genes were performed to identify the key proteins interacting with bonducellin. Molecular docking and 100 ns molecular simulations were carried out to evaluate the binding affinity and conformational stability of bonducellin with the target proteins. Additionally, the acute toxicity of bonducellin was assessed on zebrafish embryos and *in vivo* gene expression studies were performed to examine its regulatory effect on the top co-targeted gene. **Results:** The intersection of bonducellin-associated and PCOS-related genes identified 76 co-targeted genes. KEGG pathway analysis revealed their involvement in 15 critical pathways, including steroid hormone biosynthesis. Protein-protein interaction and pathway enrichment analysis highlighted key targets, including MMP9, AR, KDR, PRKACA, KIT, CYP19A1, HSD11B1, ESR1, STAT3, ESR2, PRKCA, ROCK1, BRAF, HSD17B2, PIK3R1, and RAF1, all of which exhibited strong binding to bonducellin. Molecular simulations confirmed the stability of bonducellin to the top proteins, MMP9 and AR, with high binding scores. Acute toxicity studies in zebrafish embryos determined the LC_{50} value of bonducellin as 0.8 µg/mL at 48 hpf. Gene expression analysis revealed that bonducellin differentially regulates the *MMP9* gene that is involved in modulating PCOS-related pathways. **Conclusion:** This study suggests potential gene pathways and protein interactions through which bonducellin could exert therapeutic effects on PCOS and its associated disorders. This provides valuable insights for future research into understanding and developing bonducellin-based treatments for PCOS.

Keywords: bonducellin; *Caesalpinia bonducella*; homoisoflavonoid; molecular dynamics simulation; network pharmacology; polycystic ovary syndrome; zebrafish embryo toxicity

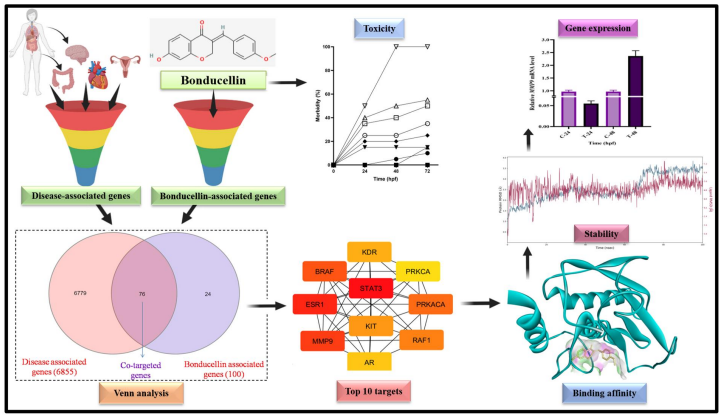

Highlights

This study elucidates the molecular mechanisms of bonducellin, a homoisoflavonoid from *Caesalpinia bonducella*, in the treatment of polycystic ovary syndrome (PCOS) through an integrated network pharmacology approach.

Molecular docking and dynamics simulations confirm bonducellin's strong and stable interactions with key PCOS-related targets, including MMP9 and AR, suggesting its role in hormone regulation and ovarian function.

Zebrafish embryo toxicity assay determined the LC_{50} of bonducellin at 0.8 µg/mL (48 hpf), with gene expression analysis revealing its modulation of *MMP9*, highlighting its potential in ovarian remodeling and extracellular matrix regulation.

The findings provide a strong theoretical foundation for future *in vivo* and clinical investigations, supporting bonducellin as a promising natural therapeutic for PCOS management.

Medical history of the objective

Caesalpinia bonducella has been widely used in Ayurvedic and Siddha medicine for centuries to treat menstrual irregularities, inflammation, and metabolic disorders. The formulation involving the seed kernel powder, which is traditionally combined with *Piper nigrum* L. and *Mel* and administered for 48 days to regulate menstrual cycles and enhance fertility, is prescribed in "*The Ayurvedic Pharmacopoeia of India*" (Part I, Volume V). These practices are rooted in ancient Ayurvedic texts such as the *Charaka Samhita* and *Sushruta Samhita* (600–200 B.C.E.), compiled by the sages Charaka and Sushruta. The plant is known for its anti-androgenic, anti-estrogenic, and metabolic regulatory properties. Bonducellin, a homoisoflavonoid from *C. bonducella,* has gained interest for its hormonal modulation, anti-inflammatory, and metabolic benefits. Traditional usage aligns with modern pharmacological findings, confirming its role in ovarian steroidogenesis, androgen regulation, and insulin signaling. Current research validates its therapeutic potential in PCOS, reproductive health, and metabolic disorders, paving the way for further clinical applications.

Background

Polycystic ovary syndrome (PCOS) is an endocrine, reproductive, and psychological condition that is becoming a global threat to women of reproductive age. It is characterized by oligo/anovulation, hyperandrogenism, polycystic ovaries, irregular menstruation, elevated luteinizing hormone (LH) to follicle-stimulating hormone (FSH) ratio, low sex hormone-binding globulin, and chronic low-grade inflammation [1]. PCOS is often associated with insulin resistance, obesity, obesity-related cardiometabolic disorders, type 2 diabetes mellitus, inflammation, and hyperleptinemia, with a global prevalence of 8 to 13% [2–5].

Currently, hormonal imbalances in women with PCOS are often treated with combined contraceptive pills, while insulin resistance is commonly managed with metformin [5, 6]. However, these treatments only provide symptomatic relief and do not address the root cause of PCOS. In many South Asian countries, PCOS is managed using a variety of herbal plants and natural ingredients, offering a complementary approach to conventional therapies [7].

Hundreds of medicinal herbs known for their beneficial effect on PCOS are being used globally [8]. For instance, *Aloe* has been traditionally prescribed by Siddha practitioners for PCOS. *Glycyrrhizae Radix et Rhizoma* and *Cinnamomi Cortex* are also recommended due to their notable effects on hormonal balance and insulin resistance [9, 10]. Supplementation of *Lini Semen* showed significant effects on hirsutism, insulin resistance, obesity, and testosterone serum concentrations [11]. Consumption of *Urticae Folium* increased circulating sex hormone-binding globulin levels and decreased androgen levels [12]. *Viticis Negundo Folium* has been used to treat anovulation and amenorrhea, while *Trigonellae Semen* has been shown to improve ovarian function and fertility [13, 14]. *Nigellae Semen* seeds decreased insulin resistance, lipid, and triglyceride levels. Phytocompounds of *Saraca asoca* were identified to possess anti-androgenic, anti-estrogenic, and anti-aromatase potential against PCOS [15, 16].

Recently, *Caesalpinia bonducella* Roxb. has gained attention for its anti-estrogenic and anti-androgenic properties [17]. In addition, it is recognized for its antibacterial, anti-diabetic, anti-inflammatory, antioxidant, hypolipidemic, and anti-cancer effects [18–21]. *Caesalpinia bonducella* has been used in ancient periods for the treatment of various ailments, including diabetes and amenorrhea, which are closely related to PCOS. The Siddha practitioners prepare it by combining *C. bonducella* seed kernel powder with pepper powder (1:3) and administering it with ghee or honey for 48 days to manage PCOS symptoms [22]. A recent investigation revealed that the ethanolic seed extracts of *C. bonducella* can restore ovarian function in mifepristone-induced PCOS rat models by modulating insulin and insulin-like growth factor pathways. Additionally, these extracts have shown potential in reducing the hyperglycemia and dyslipidemia associated with PCOS [22].

The therapeutic benefits of *C. bonducella* seed from its rich array of bioactive phytochemicals, including bonducellin, nandrolone, caesalpinin, campesterol, and carpesterol [17]. Homoisoflavonoids are one of the natural products reported for their various biological properties, which include anti-oxidant, anti-diabetic, and anti-inflammatory activities [23]. Bonducellin [(3E)-7-hydroxy-3-[(4-methoxyphenyl)methylidene]chromen-4-one] is a bioactive compound primarily found in many species of the Fabaceae family, including *Caesalpinia pulcherrima*, *Caesalpinia minax*, and *Caesalpinia millettii* [24–26]. It exhibits a range of therapeutic properties, such as anti-cancer, anti-inflammatory, anti-malarial, and anti-diabetic activities [27–29]. Recently, bonducellin has been characterized for its anti-estrogenic properties [30]. However, the molecular mechanism of its action remains to be explored.

Network pharmacology – a breakthrough discipline grounded in systematic biology and network analysis – offers practicable and reliable methods to investigate putative molecular mechanisms beyond the limitations of the conventional one-drug, one-target, one-pathway research approach [31, 32]. Leveraging the synergies between bioactive herbal substances and potential disease targets, network pharmacology approaches elucidate probable mechanisms and identify critical targets through network topological analysis [33, 34]. This strategy can also detect synergistic effects of active compounds, ultimately assisting clinical practitioners in developing rational herbal formulations [35, 36]. Molecular docking and simulation facilitate the estimation of affinity between drugs and their targets and indicate the stability of the docked complexes. Zebrafish embryos are widely employed to determine the safe dosage and toxicity of a drug or compound [37].

The present study aims to elucidate the potential mechanism of bonducellin in treating PCOS and its secondary symptoms. We performed a network pharmacology analysis and predicted binding affinities through molecular docking. The flexibility and stability of the docked complexes were assessed using molecular dynamics (MD) simulations. The toxicity of bonducellin was tested in zebrafish embryos, and the expression of the top co-targeted gene was analyzed.

Materials and methods

ADME analysis and target prediction

The ADME property of bonducellin was checked using the pharmacokinetic tool, Swiss ADME, and the probable gene targets of bonducellin were obtained using the database Swiss target prediction server (http://www.swisstargetprediction.ch/) [38]. The canonical Simplified Molecular Input Line-Entry System computed by OEChem 2.3.0 (obtained using the PubChem database – https://pubchem.ncbi.nlm.nih.gov/) was used as an input to the Swiss

target prediction server [39]. Similarly, the target gene associated with PCOS and its symptomatic disorders such as diabetes, insulin resistance, obesity, ovarian cancer, metabolic syndrome, endometrial cancer, and inflammation were identified using the DisGeNET (https://www.disgenet.org/) database, which is one of the largest databases containing information on human diseases and their associated gene targets [40]. To obtain the co-targeted genes, a Venn analysis was conducted between bonducellin targets and disease-associated genes using the InteractiVenn online tool (https://www.interactivenn.net/). Four Python programming languages were used to conduct a Venn analysis using a Jupyter notebook. The modules in Pandas were used to preprocess (dropping duplicates, empty cells, and set operations) the data, and the modules matplotlib and matplot_venn were used for data visualization. The co-targeted genes, identified through Venn analysis, were further analyzed for Protein-Protein Interactions (PPI) and Gene Ontology (GO) enrichment.

PPI, network construction

The co-targeted genes obtained by Venn analysis were given as input to the STRING database version 11.0 (https://string-db.org/), and the biological species was set to "*Homo sapiens*", with the minimum interaction threshold set to a confidence level of 0.950 to obtain the concise co-targeted protein genes that interact with bonducellin-target and disease-target genes [41]. The nodes represent the co-targeted genes, which are connected by edges (lines) that signify interactions between the nodes. All other settings were maintained at their default values to obtain PPI networks. The PPI network was further analyzed using Cytoscape version 3.10.1 along with the CytoHubba extension to identify the top-scoring targets [42, 43]. These top-scoring genes were subsequently selected for molecular docking studies.

Gene Ontology (GO) and Kyoto Encyclopedia of Genes and Genomics (KEGG) pathway enrichment analyses

The GO enrichment analysis for biological process, cell component, and molecular function was performed using STRING (version 11.0) and DAVID (https://david.ncifcrf.gov/), the databases that offer systematized and extensive functional annotation for large-scale genes or proteins. The co-targeted genes were given as inputs, and the species was set to "*Homo sapiens*" with a threshold value of $P \leq 0.05$ for GO enrichment. The SR plot (https://www.bioinformatics.com.cn/en) was employed to generate the bubble and bar plots. The top 15 pathways relevant to PCOS from the KEGG pathway and GO enrichment were taken for further analysis.

Molecular docking

Based on the PPI and KEGG pathway analysis from the network pharmacology report, 16 major target proteins were selected, and their crystal structures were obtained from the Protein Data Bank (PDB) (https://www.rcsb.org/): MMP9 (PDB: 6ESM), AR (PDB: 5JJM), KDR (PDB: 3WZE), PRKACA (PDB: 1Q8U), KIT (PDB: 6ITT), CYP19A1 (PDB: 5JKV), HSD11B1 (PDB: 4BB5), ESR1 (PDB: 2QE4), STAT3 (PDB: 6NUQ), ESR2 (PDB: 3OLL), PRKCA (PDB: 3IW4), ROCK1 (PDB: 3V8S), BRAF (PDB: 7MED), HSD17B2 (PDB: 7X3Z), PIK3R1 (PDB: 8DCP), and RAF1 (PDB: 7Z38) [44–59]. The selection criteria of the protein structure, including uniport ID, full form of the protein, experimental methods, resolution, organism, and mutations, are detailed in Supplementary Table S1. The files were desolvated and dehydrated using PyMOL 2.6 software (https://www.pymol.org/), hydrogenated, converted to pdbqt format using Autodock 4.2.6 software (https://autodock.scripps.edu/), and subsequently used for molecular docking. Ligand preparation was performed using the Autodock tool, where a torsion tree was used to determine the root expansion, and the ligand was converted to pdbqt format. The detailed docking parameters, including grid box dimensions and binding site information, are provided in Supplementary Table S2. The docking score is represented in kcal/mol. Following docking, the PLIP online tool (https://plip-tool.biotec.tu-dresden.de/plip-web/plip/index) was used to identify the bond interactions (hydrogen, hydrophobic bonds) of the protein-ligand complex obtained from Autodock. Finally, Discovery Studio Visualizer v21.1.0.20298 (https://www.3ds.com/products/biovia/discovery-studio) was used to visualize and obtain 2D and 3D representative illustrations of the protein-ligand interactions.

Molecular dynamics simulation

The Desmond 2023.2 module (https://www.schrodinger.com/platform/products/desmond/) (academic version) was used to perform MD simulations [60–62]. PyMOL was used to export the ligand-protein complex's three-dimensional model to the PDB file format. The complex was introduced into the system. With periodic boundary conditions, it was solvated using the Transferable Intermolecular Potential with 3 Points water model in a cubic box that was more than 1 nm from the protein's edge. The steepest descent approach was used to minimize energy over a 50,000-step period after injecting Na^+ ions to neutralize the system. The system was subsequently brought to equilibrium using 100 ps of NVT simulation at 300 K and 100 ps of NPT simulation. The constant temperature (NVT) and constant pressure (NPT) ensembles used the leapfrog method to link each component, such as proteins, ligands, water molecules, and ions, separately. The system was maintained in a stable environment (300 K temperature and 1 bar pressure) by using the Berendsen temperature and pressure coupling constants. Then, an MD simulation was run in an isothermal and isobaric condition ensemble at 300 K for 100 ns.

The trajectory file was analyzed using the simulation interaction diagram, encompassing multiple attributes of the dynamic studies such as protein-ligand root mean square deviation (RMSD), protein and ligand root mean square fluctuation (RMSF), ligand torsion profile, protein-ligand contacts, as well as ligand-protein contacts with respect to time.

Zebrafish embryo toxicity

Bonducellin was chemically synthesized in our laboratory, following the scheme previously reported in our study [63]. The stock solution was prepared in 0.1% DMSO (Sisco Research Laboratories Pvt, Ltd., Mumbai, India). Zebrafish embryos used in the study were obtained from Tarun Fish Farm, Chennai, India (Registration No: FWCS-80). The embryos were maintained under standard laboratory conditions with proper temperature, light/dark cycle, and water quality controls. All animal experiments were conducted as per institutional guidelines and adhered to Good Laboratory Practice (GLP) standards, ensuring a controlled and hygienic environment for all procedures. The zebrafish embryo toxicity assay was performed following the OECD guidelines for testing chemicals, acute toxicity test, OECD 203 (1992). To ensure uniformity, the embryos were stage-selected and exposed to the compound throughout embryogenesis from 2 hpf, continuing until 72 hpf. Bonducellin was tested at concentrations of 0.1, 0.25, 0.5, 0.75, 1, 2.5, and 5 μg/mL with 0.1% DMSO as vehicle control. The experiment was conducted in 24-well plates with one embryo per well, containing 1 ml of working solution prepared in E3 medium. Each experimental and control group contained 20 embryos, and the toxicity test was conducted under static conditions. Embryos were monitored at 24, 48, and 72 hpf for mortality and developmental malformations, and the percentage of mortality over time was calculated. The LC_{50} values were calculated according to the Litchfield-Wilcoxon method [64].

Gene expression analysis in zebrafish embryos

Zebrafish embryos were seeded in 24-well plates following the same protocol as described above. After the bonducellin treatment (LC_{50} dose) for 24 and 48 h, the embryos were washed twice with phosphate-buffered saline. Total RNA was extracted from bonducellin-treated embryos using RNA IsoPlus (Takara, Kusatsu, Japan). Following the manufacturer's protocol, complementary DNA (cDNA) was synthesized using the cDNA synthesis kit (Bio-rad, Hercules, CA, USA) with 1 μg of total RNA as the template. The cDNA synthesis reaction was performed under the following conditions: 25

°C for 5 min, reverse transcription at 46 °C for 20 min, and enzyme inactivation at 95 °C for 1 min.

The synthesized cDNA was used for reverse transcription polymerase chain reaction (RT-PCR) amplification of the targeted genes. The list of primers used for the RT-PCR is provided in Table 1. The PCR reaction was carried out under the following conditions: initial denaturation at 95 °C for 5 min, followed by 28 cycles of denaturation at 95 °C for 30 s, annealing at 58 °C for 30 s, and extension at 72 °C for 30 s, with a final extension of 72 °C for 1 min. PCR products were separated on a 1% agarose gel and visualized under UV light, and the image was captured in inverted mode. Gene expression levels were quantified using ImageJ 1.30v software (https://imagej.net/ij/) and normalized to the housekeeping gene *β-Actin* [65].

Statistical analysis

Statistical analysis was performed using GraphPad Prism version 9.3.1 (https://www.graphpad.com/features), with all experiments conducted in triplicate. Data are expressed as mean ± SD. Differences between treated and control groups were evaluated using Student's t-test, and statistical significance was set at $^{*}P < 0.05$, $^{**}P < 0.01$.

Results

Drug-likeliness of bonducellin

Bonducellin adheres to Lipinski's rule of five, which is important for evaluating its drug-like properties. Bonducellin, with a molecular weight of 282.29 g/mol, plays a crucial role in determining its physical and chemical characteristics, thereby influencing solubility, permeability, and overall pharmacokinetic behaviour. This factor is essential in drug development as it impacts dosage, bioavailability, and metabolic processes. The compound contains 21 heavy atoms, 12 of which are aromatic, highlighting its structural complexity and aromaticity. A higher number of heavy atoms typically indicates a more intricate structure, while the presence of aromatic heavy atoms can affect chemical reactivity. Additionally, bonducellin's low fraction of sp^3-hybridized carbon atoms (0.12) suggests a predominance of aromatic or unsaturated characteristics, which may influence its stability and reactivity in biological systems.

With only 2 rotatable bonds, bonducellin appears relatively rigid, a crucial aspect in drug design where flexibility can impact binding affinity and pharmacokinetic properties. Bonducellin's 4 hydrogen bond acceptors and 1 donor provide insights into potential interactions with biological molecules, which is crucial for understanding its ability to form hydrogen bonds, especially in drug-receptor interactions. With a molar refractivity of 79.14 and a Topological Polar Surface Area of 55.76 $Å^2$, bonducellin's physicochemical properties related to polarizability and surface area contribute to understanding its solubility, permeability, and interaction with biological membranes. Bonducellin exhibits high gastrointestinal absorption and permeability across the blood-brain barrier, suggesting potential oral bioavailability and central nervous system effects. Not being a P-gp substrate enhances its chances of successful absorption.

The Log K_P value (−5.93 cm/s) for bonducellin indicates poor skin permeation, a feature that may be desirable depending on its intended use, such as avoiding transdermal absorption. Bonducellin's LD_{50} value of 3,800 mg/kg provides information about its acute toxicity, critical for assessing the compound's safety for therapeutic use. The physicochemical and pharmacokinetic parameters of bonducellin are given in Table 2, and the bioavailability radar of bonducellin is presented in Supplementary Figure S1.

Target prediction

The canonical Simplified Molecular Input Line-Entry System of bonducellin submitted into the Swiss target prediction tool uncovered 100 gene targets of the phytocompound in *Homo sapiens*. A total of 6,855 disease gene targets associated with PCOS and its symptomatic disorders, such as diabetes, insulin resistance, obesity, ovarian cancer, metabolic syndrome, endometrial cancer, and inflammation, were retrieved from the DisGeNET database. The Venn analysis of the 100 bonducellin-associated genes and the 6,855 disease-associated genes identified 76 co-targeted genes or hub genes, as displayed in Figure 1 (Supplementary Tables S3, S4).

Table 1 List of primers used in RT-PCR

S. No.	Gene	Forward primer	Reverse primer
1	*MMP9*	5'TTGGCTTCTGTCCCAGTGAG3'	5'TTAGGGCAGAATCCATACTT3'
2	*β-Actin*	5'TGGCATCACACCTTCTAC3'	5'AGACCATCACCAGAGTTC3'

MMP9, Matrix Metalloproteinase-9.

Table 2 Physicochemical and pharmacokinetic parameters of bonducellin

S. No	Parameters	Range
1	Formula	$C_{17}H_{14}O_4$
2	Molecular weight	282.29 g/mol
3	No. of heavy atoms	21
4	No. of aromatic heavy atoms	12
5	Fraction Csp^3	0.12
6	No. rotatable bonds	2
7	No. of H-bond acceptors	4
8	No. of H-bond donors	1
9	Molar Refractivity	79.14
10	TPSA	55.76 $Å^2$
11	GI absorption	High
12	BBB permeant	Yes
13	P-gp substrate	No

Table 2 Physicochemical and pharmacokinetic parameters of bonducellin (*continued*)

S. No	Parameters	Range
14	CYP1A2 inhibitor	Yes
15	CYP2C19 inhibitor	Yes
16	CYP2C9 inhibitor	No
17	CYP2D6 inhibitor	No
18	CYP3A4 inhibitor	Yes
19	Log K_p (skin permeation)	−5.93 cm/s
20	Toxicity class	5
21	LD_{50}	3,800 mg/kg

GI, gastrointestinal; BBB, Blood-Brain Barrier; TPSA, Topological Polar Surface Area; LD_{50}, lethal dose 50.

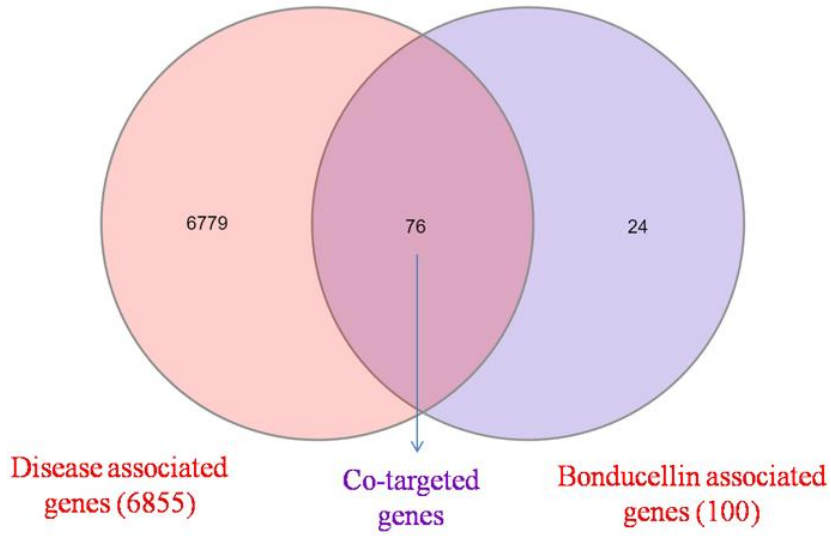

Figure 1 Venn analysis performed using bonducellin-associated targets and disease-associated targets representing co-targeted genes

PPI network construction and GO enrichment

The co-targeted genes imported into the STRING platform provided PPI information among the hub genes (Figure 2). GO enrichment analysis of these co-targeted genes identified a total of 299 GOs associated with the therapeutic effects of bonducellin on PCOS and its symptomatic disorders (Supplementary Table S5), which were categorized into three main categories: 1. Biological processes: two GOs were identified, including collagen degradation and apoptosis, with gene counts of 4 and 9, respectively. 2. Cellular components: six GOs were identified, including cell membrane, membrane, cytoplasm, cell projection, endoplasmic reticulum, and extracellular matrix, with gene counts of 31, 48, 36, 11, 11, and 4, respectively. 3. Molecular functions: eight GOs were identified, including kinase, serine/threonine-protein kinase, tyrosine-protein kinase, transferase, metalloprotease, receptor, hydrolase, and oxidoreductase, with gene counts of 30, 20, 11, 30, 6, 20, 19, and 9, respectively. These results are illustrated as a bar graph in Figure 3. The results obtained from the PPI network of the co-targeted genes *STAT3, MMP9, ESR1, BRAF, PRKACA, RAF1, KIT, KDR, AR,* and *PRKCA* showed the highest degree of overlapping, given in Supplementary Table S6 and the top targets are represented in Figure 4.

KEGG pathway enrichment analysis

The KEGG pathway enrichment analysis identified the top 15 signaling pathways (Figure 5) involved in the probable mechanism by which bonducellin treatment can affect PCOS and its symptomatic disorders among the 106 signaling pathways (Supplementary Table S7). The results suggested that co-targeted genes are mainly associated with steroid hormone biosynthesis, the gonadotropin-releasing hormone (GnRH) signaling pathway, the estrogen signaling pathway, and insulin resistance, which participate in the etiology of PCOS.

Molecular docking

Based on the enrichment analysis, the top 16 gene targets associated with PCOS and its symptomatic disorders- MMP9, AR, KDR, PRKACA, KIT, CYP19A1, HSD11B1, ESR1, STAT3, ESR2, PRKCA, ROCK1, BRAF, HSD17B2, PIK3R1, and RAF1 proteins- were subjected to molecular docking against bonducellin to identify their binding affinity. These docking scores reflect the predicted strength of the binding interactions between the mentioned proteins and bonducellin. Lower scores generally indicate a stronger binding affinity. The amino acid residues listed are likely involved in the binding sites or regions responsible for the interactions between the proteins and their ligands. The information presented here is valuable for understanding the molecular details of these interactions, which can have implications for drug discovery and design. The binding scores of the bonducellin towards the major targets are given in Table 2. The docking images of the two high-affinity proteins, MMP9 and AR, are presented in Figure 6.

Molecular dynamics simulations

To understand the conformational changes and evaluate the binding stability of bonducellin in a solvent atmosphere against top-scoring MMP9 and AR proteins, we have carried out MD simulations for a period of 100 ns for two complexes, namely bonducellin-MMP9 and bonducellin-AR protein complex. Their simulations were evaluated using various statistical parameters, including RMSD of apoproteins and protein-ligand complexes, RMSF of proteins and ligands, radius of gyration, and protein-ligand interactions over time from the obtained trajectory.

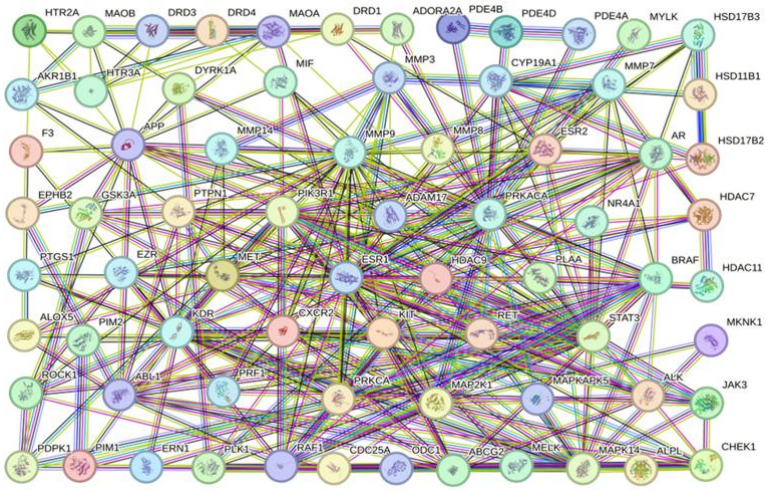

Figure 2 PPI network of co-targeted genes of bonducellin-associated targets and disease-associated targets. HTR2A, serotonin 2a receptor; MAOB, monoamine oxidase B; DRD3, dopamine D3 receptor; DRD4, dopamine D4 receptor; MAOA, monoamine oxidase A; DRD1, dopamine D1 receptor; ADORA2A, adenosine A2A receptor; PDE4B, phosphodiesterase 4B; PDE4D, phosphodiesterase 4D; PDE4A, phosphodiesterase 4A; MYLK, myosin light chain kinase; HSD17B3, estradiol 17-beta-dehydrogenase 3; AKR1B1, aldose reductase; HTR3A, serotonin 3A receptor; DYRK1A, dual-specificity tyrosine-phosphorylation regulated kinase 1A; MIF, macrophage migration inhibitory factor; MMP3, matrix metalloproteinase 3; CYP19A1, cytochrome P450 19 subfamily A member 1; MMP7, matrix metalloproteinase 7; HSD11B1, 11-beta-hydroxysteroid dehydrogenase 1; F3, coagulation factor III/tissue factor; APP, amyloid beta precursor protein; MMP14, matrix metalloproteinase 14; MMP9, matrix metalloproteinase 9; MMP8, matrix metalloproteinase 8; ESR2, estrogen receptor beta; AR, androgen receptor; HSD17B2, estradiol 17-beta-dehydrogenase 2; EPHB2, Ephrin type-B receptor 2; GSK3A, glycogen synthase kinase-3 alpha; PTPN1, protein-tyrosine phosphatase, non-receptor type 1; PIK3R1, phosphoinositide-3-kinase regulatory subunit 1 (p85-alpha); ADAM17, A disintegrin and metalloprotease 17; PRKACA, protein kinase cAMP-activated catalytic subunit alpha; NR4A1, nuclear receptor subfamily 4 group A member 1; HDAC7, histone deacetylase 7; PTGS1, prostaglandin endoperoxide synthase 1 (Cyclooxygenase-1); EZR, Ezrin; MET, Met proto-oncogene, receptor tyrosine kinase (hepatocyte growth factor receptor); ESR1, estrogen receptor alpha; HDAC9, histone deacetylase 9; PLAA, phospholipase A2-activating protein; BRAF, serine/threonine-protein kinase B-Raf; HDAC11, histone deacetylase 11; ALOX5, Arachidonate 5-lipoxygenase; PIM2, serine/threonine-protein kinase PIM2; KDR, kinase insert domain receptor (vascular endothelial growth factor receptor 2); CXCR2, C-X-C motif chemokine receptor 2 (interleukin-8 receptor B); KIT, KIT proto-oncogene receptor tyrosine kinase (stem cell growth factor receptor); RET, RET proto-oncogene receptor tyrosine kinase; STAT3, signal transducer and activator of transcription 3; MKNK1, MAP kinase-interacting serine/threonine-protein kinase MNK1; ROCK1, Rho-associated protein kinase 1; ABL1 proto-oncogene 1, non-receptor tyrosine kinase; PRF1, perforin 1; PRKCA, protein kinase C alpha; MAP2K1, mitogen-activated protein kinase 1; MAPKAPK5, MAP kinase-activated protein kinase 5; ALK, anaplastic lymphoma kinase; JAK3, Janus kinase 3; PDPK, 3-phosphoinositide dependent protein kinase-1; PIM1, serine/threonine-protein kinase PIM1; ERN1, endoplasmic reticulum to nucleus signaling 1 (serine/threonine-protein kinase/endoribonuclease IRE1); PLK1, Polo-like kinase 1; RAF1, RAF proto-oncogene serine/threonine-protein kinase; CDC25A, cell division cycle 25A; ODC1, Ornithine decarboxylase 1; ABCG2, ATP-binding cassette sub-family G member 2; MELK, maternal embryonic leucine zipper kinase; MAPK14, mitogen-activated protein kinase 14 (p38 alpha); ALPL, alkaline phosphatase, tissue-nonspecific isozyme; CHEK1, checkpoint kinase 1 (serine/threonine-protein kinase Chk1).

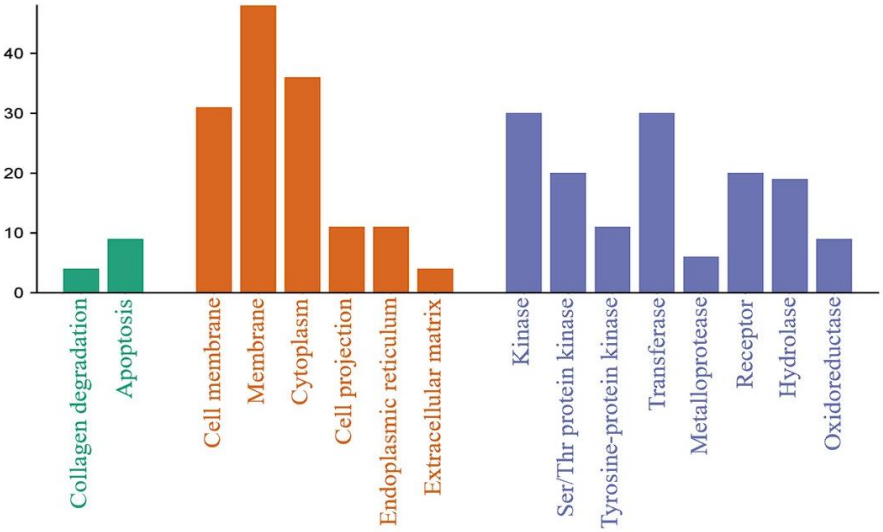

Figure 3 GO enrichment analysis chart of the BP (green), CC (orange), and MF (Blue) categories from GO enrichment analysis. The X-axis and Y-axis show the gene count and full name of the processes, respectively. BP, biological process; CC, cellular components; MF, molecular function.

Traditional Medicine Research 2025;10(11):65. https://doi.org/10.53388/TMR20241216001

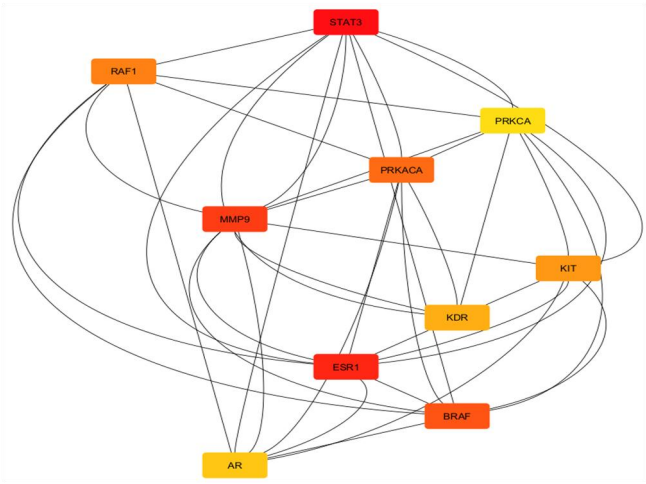

Figure 4 Top 10 ranked genes based on the PPI network of co-targeted genes. MMP9, Matrix Metalloproteinase-9; RAF1, Raf-1 Proto-Oncogene (Serine/Threonine Kinase); STAT3, Signal Transducer and Activator for Transcription 3; PRKCA, protein kinase C alpha; PRKACA, protein kinase cAMP-activated catalytic subunit alpha; KDR, Kinase Insert Domain Receptor; KIT, Protooncogene C KIT (Tyrosine Protein Kinase); AR, androgen receptor; BRAF, B-Raf proto-oncogene (serine/threonine-protein kinase); ESR1, estrogen receptor 1.

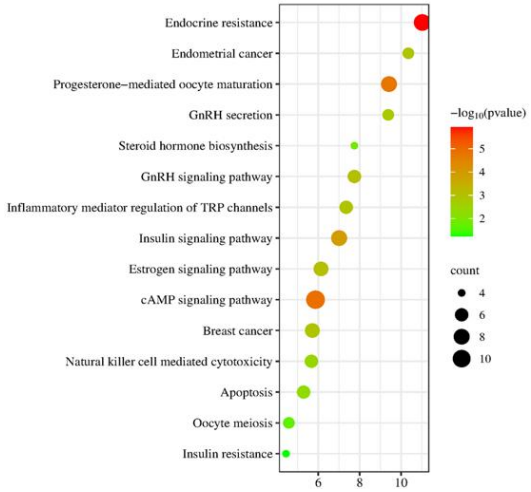

Figure 5 KEGG pathway enrichment analysis of the top fifteen signaling pathways by gene ratio and their target genes related to PCOS and its symptomatic disorders based on KEGG pathway. GnRH, gonadotropin-releasing hormone.

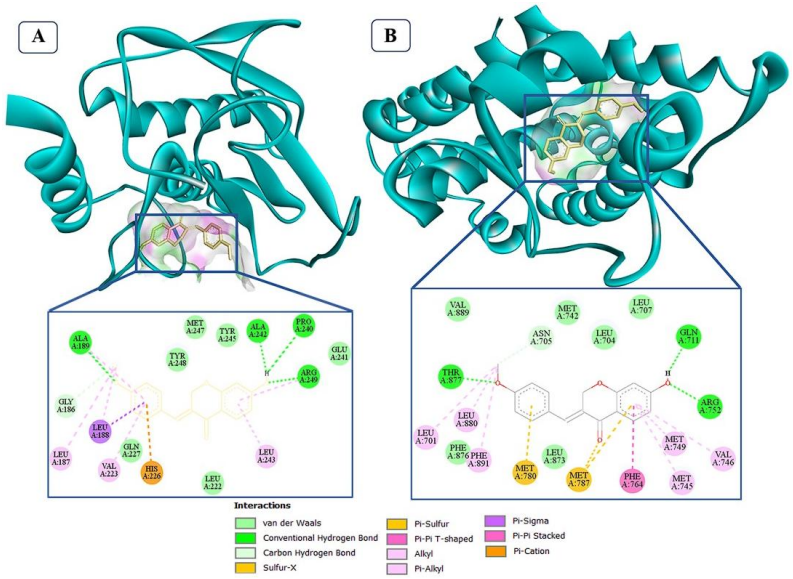

Figure 6 Molecular docking of bonducellin against key target proteins with their 2D structure of the binding sites. (A) MMP9 (PDB: 6ESM) docked with bonducellin. (B) AR (PDB: 5JJM) docked with bonducellin.

After the simulation, RMSD was utilized to understand the structural conformation of the ligand and protein. Figure 7 displays the RMSD (Å) vs time multiplot for bonducellin-MMP9 and bonducellin-AR protein complex (pink) simulations along with their apoproteins (blue). The apo-MMP9 protein stabilized at an RMSD of 2.5–2.8 Å, while the bonducellin-MMP9 complex displayed fluctuation till 60 ns up to 1.2 Å, after which the trajectory attained a stable RMSD between 2.8 and 3.2 Å. The ligand RMSD initially fluctuated around 3.5 Å for the first 15 ns but stabilized between 2.6 and 3.0 Å, indicating strong retention in the binding pocket. Similarly, the apo-AR protein reached RMSD stability around 2.0 Å, while the bonducellin-AR complex displayed deviation in 40 ns between 1.2 and 1.8 Å, increasing to 2.1 Å in 60 ns, followed by stabilization at 2.1 Å till 100 ns. This minor deviation in both MMP9 and AR bonducellin complexes throughout indicates excellent stability, with MMP9 being more stable than AR protein.

Characterizing local alterations throughout the protein chain is done with the protein RMSF. Figure 8 displays the protein-RMSF (Å) vs residue number index multiplot. The protein RMSF of bonducellin-MMP9 was less than 2.7 Å for all amino acid residues except the residues from 60 to 65, which had an RMSF of 5.6 Å. Similarly, the protein RMSF of the bonducellin-AR complex was less than 2.5 Å for all amino acid residues except the residues from 150 to 155, which had an RMSF of 3.2 Å. However, these fluctuations are not located in the ligand's binding site, suggesting that they do not impact ligand stability.

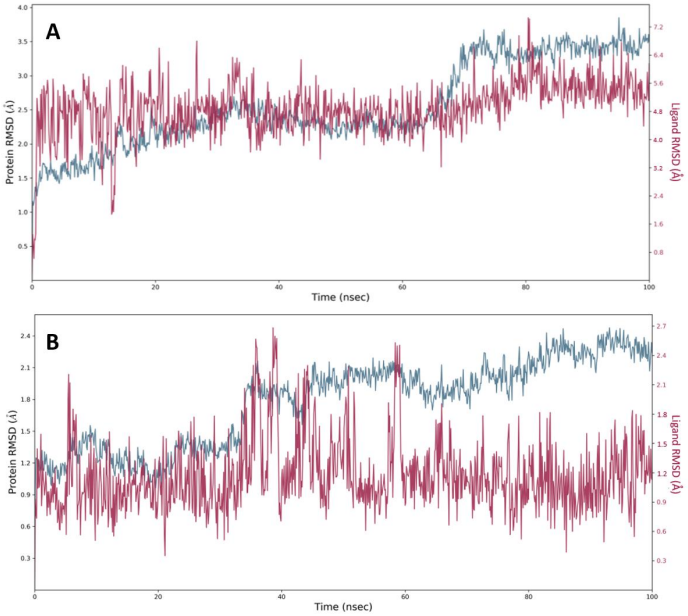

Figure 7 Graphical representation of the plots showing RMSD (Å) versus time (100 ns). (A) Bonducellin-MMP9 complex RMSD. (B) Bonducellin-AR complex RMSD. blue represents apoprotein; pink represents protein-ligand complex. RMSD, root-mean-square deviation.

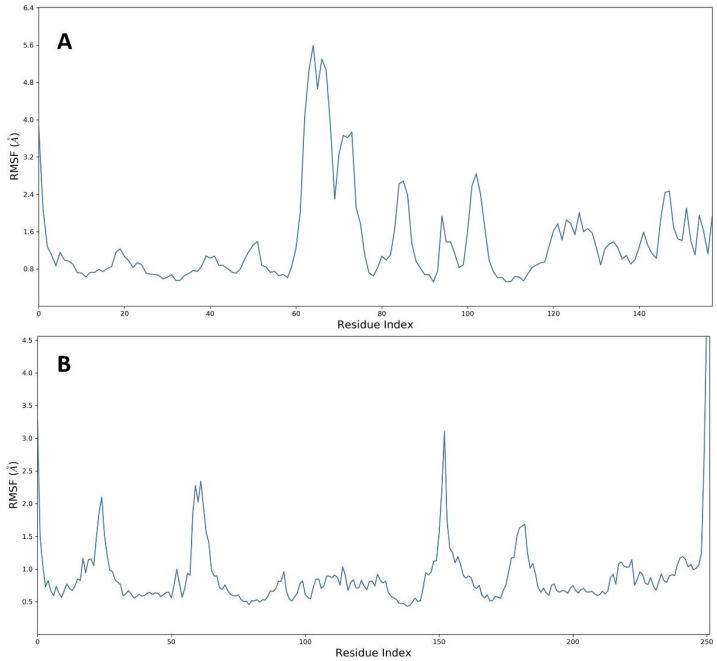

Figure 8 Graphical representation of the plots showing the protein RMSF (Å) versus residue index number of protein. (A) Bonducellin-MMP9 complex protein. (B) Bonducellin-AR complex protein. RMSF, root mean square fluctuation.

Solvent-accessible surface area analysis showed a stable protein-solvent exposure, with total solvent-accessible surface area values fluctuating between 7,500–7,800 Å^2 for MMP9 and 9,500–9,800 Å^2 for AR, confirming no major solvent-induced collapse (Figure 9). The ligand interaction fractions of bonducellin with the amino acids of MMP9 and AR during the span of 100 ns are depicted in Figure 10. As shown in Table 3, the bonducellin-MMP9 complex exhibited 8 hydrogen bonds and 7 hydrophobic bond interactions, where all 7 hydrophobic bonds and 4 H-bonds were observed during docking Ala189, His226, Ala242, and Arg249. However, 4 new H-bond interactions with Tyr179, Gln227, Glu241, and His257 residues were observed during MD simulations in a solvent environment, which can further facilitate the binding affinity and stability of the bonducellin-MMP9 complex. Similarly, the bonducellin-AR complex shows 5 hydrogen bonds and 17 hydrophobic bond interactions, in which only 3 H-bonds, Gln711, Arg752, and Thr877, and 5 hydrophobic bonds, Leu701, Val746, Met749, Leu873z, and Phe876, were observed during molecular docking. However, during molecular simulations, 2 new H-bonds, Asn705 and Phe764, and 12 new hydrophobic bonds Leu704, Leu 707, Met742, Met745, Phe764, Met780, Leu 873, Leu880, Val889, Phe891, Met895, and Ile899, were observed that further aid with the stable binding of bonducellin to AR. Additionally, water-bridged hydrogen bonds were observed with His226, Glu241, and Arg249 in MMP9 and Gln711, Arg752, and Thr877 in AR, reinforcing ligand stability through solvent mediation.

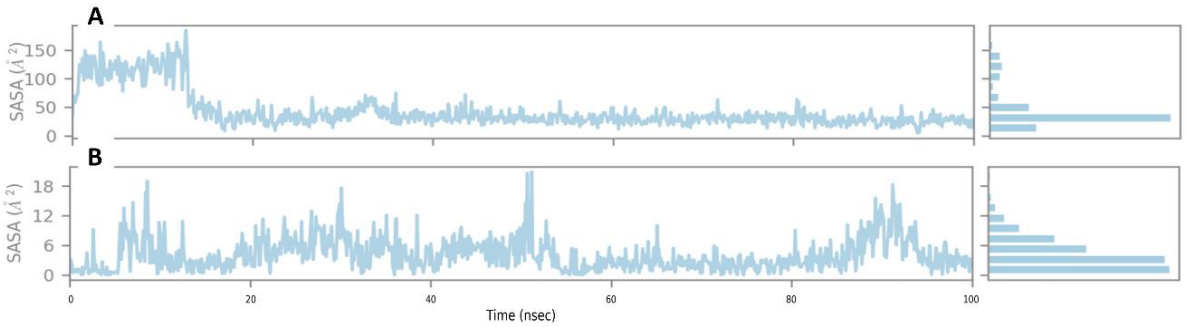

Figure 9 The SASA plots during 100 ns molecular simulation showing SASA (Å^2) versus time (ns). (A) Bonducellin-MMP9 complex. (B) Bonducellin-AR complex. SASA, solvent accessible surface area.

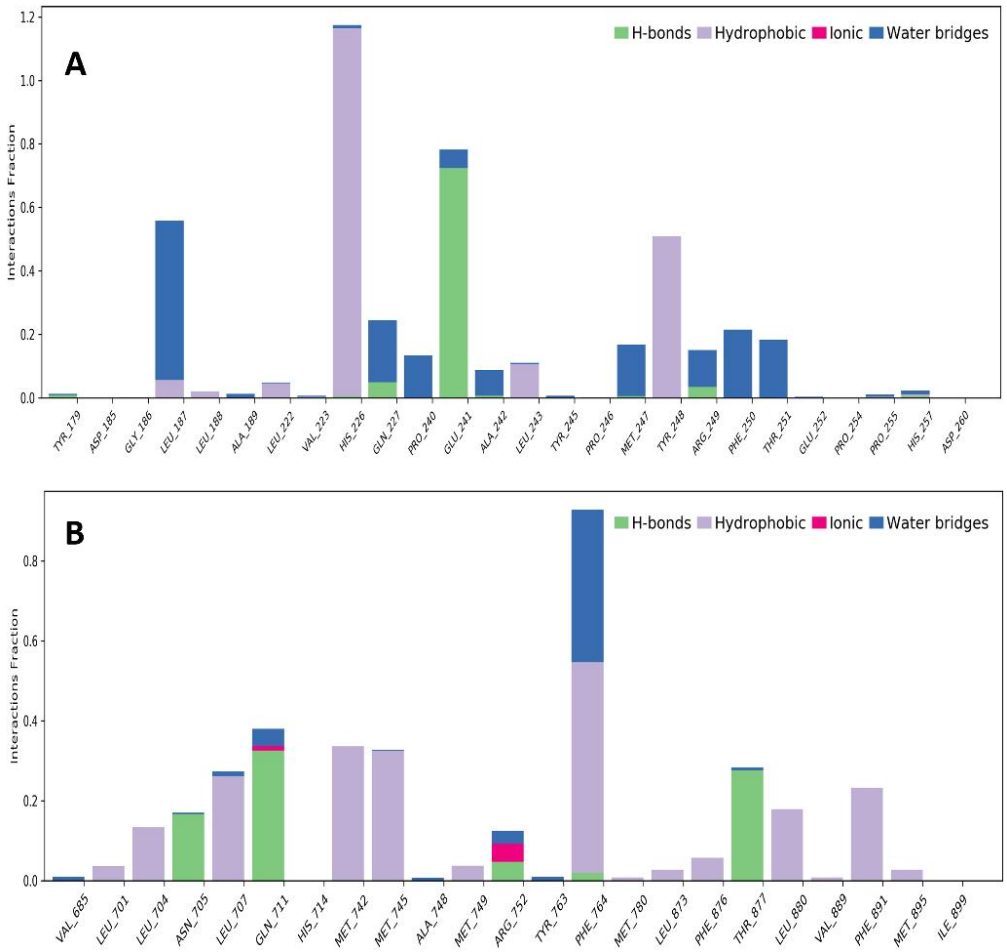

Figure 10 The histogram of protein-ligand interactions throughout the simulation trajectory. (A) Bonducellin-MMP9 contacts. (B) Bonducellin-AR contacts.

Table 3 Docking report of bonducellin against the 16 target proteins compared with their native ligands

Target proteins & PDB IDs	Associated pathway(s)	PCOS related symptom(s)	Docking score (kcal/mol)	Bonducellin		Native ligand		Reference
				Hydrogen Bond	Hydrophobic Bond	Hydrogen Bond	Hydrophobic Bond	
MMP9 (6ESM)	ECM remodeling, inflammation	Ovarian dysfunction, fibrosis	−11.25	Tyr179, His226, Gln227, Glu241, Ala242, Met247, Arg249, His257	Leu187, Leu188, Leu222, His226, Leu243, Tyr248, His260	Gln227	Leu187, His190, Val223, His226, Leu243, Tyr248	[44]
AR (5JJM)	Androgen signaling	Hyperandrogenism, hirsutism	−9.24	Asn705, Gln711, Arg752, Phe764, Thr877	Leu701, Leu704, Leu707, Met742, Met745, Val746, Met749, Phe764, Leu873, Met780, Leu873, Phe876, leu880, Val889, Phe891, Met895, Ile899	Asn795, Gln711, Arg752	Leu701, Leu707, Met745, Val746, Phe764	[45]
KDR (3WZE)	VEGF signaling	Abnormal ovarian angiogenesis	−8.8	Lys868, Cys919	Val848, Ala866, Val899, Val916, Phe918, Leu1035	Lue885, Cys919, Asp1046	Val848, Ala866, Lys868, Glu885, Leu889, Val916, Leu1035, Phe1047	[46]
PRKACA (1Q8U)	cAMP signaling	Insulin resistance, hormonal imbalance	−8.58	Asn99, Phe100, Leu106	Gln96, Asn99, Leu103, Leu106	Val123	Leu49, Ala70, Leu173, Thr183, Phe327	[47]
KIT (6ITT)	Stem cell factor signaling	Follicular development issues	−8.5	Lys623, Glu640, Gly676	Leu595, Val603, Ala621, Leu644, Thr670, Tyr672, Leu799, Phe811	Lys623, Glu640, Cys673, Asp810	Leu595, Leu647, Ile653, Tyr672, Leu783, Leu799, Asp810	[48]
CYP19A1 (5JKV)	Estrogen biosynthesis	Estrogen imbalance, menstrual irregularities	−8.29	Ser314, Val370, Pro429	Ala306, Val370, Ala443	Arg115, Met374	Trp224, Ala306, Asp309, Thr310, Val370, Leu372, Leu477	[49]
HSD11B1 (4BB5)	Cortisol metabolism	Stress-related metabolic disturbance	−7.98	Ile46, Gly47, Thr92, Met93, Asn119, Ile121	Lys44, Arg66	Gly41, Ser43, Lys44, Ile46, Arg66, Ser67, Thr92, Met93, Asn119, Ile121, Tyr183, Lys187, Ile218, Tyr220	Leu215	[50]
ESR1 (2QE4)	Estrogen receptor signaling	Endometrial dysfunction, infertility	−7.59	Glu353, Met357, Trp393, Lys449	Pro324, Ile326, Arg394	Trp393, Lys449	Pro324, Ile326	[51]

Table 3 Docking report of bonducellin against the 16 target proteins compared with their native ligands (*continued*)

Target proteins & PDB IDs	Associated pathway(s)	PCOS related symptom(s)	Docking score (kcal/mol)	Bonducellin		Native ligand		Reference
				Hydrogen Bond	Hydrophobic Bond	Hydrogen Bond	Hydrophobic Bond	
STAT3 (6NUQ)	JAK-STAT signaling	Chronic inflammation, metabolic issues	−7.32	Asp369, Lys370, Ser381, Thr440, Glu455, Lys488	Asp369, Lys370, Leu438, Thr440, Val490	Lys370, Ser381, Lys488	Thr440, Val490	[52]
ESR2 (3OLL)	Estrogen receptor signaling	Impaired ovarian function	−7.26	Glu305, Leu342, Arg346, Leu491, Leu492	Leu298, Leu301, Ala302, Phe 356, Pro486	Glu305, Arg346, His475	Leu298, Leu301, Leu343	[53]
PRKCA (3IW4)	PI3K/AKT signaling	Insulin resistance, metabolic syndrome	−7.14	His455, Gly458, Gly492, Pro514, Gly516, Lys517, Ser518	Pro577	Thr401, Glu418, Val420	Leu345, Phe350, Val353, Lys368, Ala480, Asp481	[54]
ROCK1 (3V8S)	Cytoskeletal regulation	Ovarian dysfunction, fibrosis	−7.11	Phe110, Lys114, Asn390	Lys109, Phe110, Ile113, Lys114, Thr380, Phe381	Met156, Asp216	Val90, Ala103, Lys105, Leu107, Leu205, Ala215	[55]
BRAF (7MFD)	MAPK signaling	Follicular growth abnormalities	−6.77	Cys264	Asp249, Tyr266, Arg691, Glu695	/	Tyr266, Arg691,	[56]
HSD17B2 (7X3Z)	Steroid hormone metabolism	Estrogen imbalance	−6.62	His179, Leu180	Leu174, Lys248	Tyr 155, Glu282	Val143, Leu149, Val225, Phe226, Phe259	[57]
PIK3R1 (8DCP)	PI3K/AKT signaling	Insulin resistance, obesity	−6.48	Arg348, Pro427, Ser429, Gln433	Lys346, Arg348, Val428	Pro427, Gln433	Arg348, Val428	[58]
RAF1 (7Z38)	MAPK/ERK signaling	Ovarian dysfunction, metabolic issues	−6.2	Lys53, Asp88, Gln128, Val131	/	Asn46, Asp49, Lys53, Asp88, Asn101, Ser108, Gly109, Thr110, Gln128, Phe129, Gly130, Val131, Gly132, Phe133	/	[59]

MMP9, Matrix Metalloproteinase-9; ECM, extracellular matrix; AR, androgen receptor; KDR, Kinase Insert Domain Receptor; VEGF, vascular endothelial growth factor; PRKACA, protein kinase cAMP-activated catalytic subunit alpha; cAMP, cyclic Adenosine Mono-Phosphate; KIT, Protooncogene C KIT (Tyrosine Protein Kinase); CYP19A1, cytochrome P450 family 19 subfamily A member 1 (aromatase); HSD11B1, hydroxysteroid 11-beta dehydrogenase 1; ESR1, estrogen receptor 1; ESR2, estrogen receptor 2; STAT3, Signal Transducer and Activator for Transcription 3; JAK/STAT, Janus kinase/signal transducers and activators of transcription; PRKCA, protein kinase C alpha; PI3K/AKT, phosphatidylinositol 3-kinase/protein kinase B; ROCK1, Rho-associated protein kinase 1; BRAF, B-Raf proto-oncogene (serine/threonine-protein kinase); MAPK, mitogen-activated protein kinase; HSD17B2, 17beta-hydroxysteroid dehydrogenase type 2; PIK3R1, phosphoinositide-3-kinase regulatory subunit 1; RAF1, Raf-1 Proto-Oncogene (Serine/Threonine Kinase); ERK, extracellular signal-regulated kinase; PCOS, polycystic ovary syndrome.

The protein-ligand 2D interactions of both bonducellin-MMP9 and bonducellin-AR complex following the 100 ns are depicted in Figure 11, showing that the amino acids of MMP9 and AR proteins majorly formed hydrophobic, polar, and pi-pi stacking bonds with bonducellin, where some interactions were mediated by water molecules. Figure 12 shows the ligand torsion profile of bonducellin with MMP9 and AR proteins. The profile displayed minimal torsional flexibility in MMP9, indicating a rigid and stable conformation within the pocket. In contrast, moderate fluctuations in AR suggest some flexibility, allowing bonducellin to adapt to its binding site. Figure 13 shows the radius of the gyration of the bonducellin-MMP9 and the bonducellin-AR complexes; both are stable throughout the simulation period. The radius of the gyration stability confirms that MMP9 and AR proteins remain structurally compact and stably folded over 100 ns, depicting the compactness of the proteins. These results suggest that bonducellin maintains strong and stable binding with both MMP9 and AR, with MMP9 demonstrating higher stability, making it a potential candidate for further drug development.

Zebrafish embryo toxicity

A zebrafish embryo toxicity bioassay was used to assess the developmental effects of bonducellin exposed at different concentrations (0.1, 0.25, 0.5, 1, 2.5, 5 µg/mL) with 0.1% DMSO as the vehicle control. The result demonstrated that bonducellin is effective even at lower doses, with minimal toxicity observed at a dose of 0.1–0.5 µg/mL, with a morbidity rate below 30% in all time intervals. However, a gradual increase in morbidity was observed at 0.75–5 µg/mL, with the highest concentration of 5 µg/mL showing 100% morbidity at 48 h post-fertilization, indicating a rapid and effective activity at higher doses. A significant difference was observed in the morbidity of embryos from control to treated groups, with statistical significance increasing at higher concentrations ($P < 0.05$) (Figure 14). The LC_{50} values calculated using the Litchfield-Wilcoxon method were determined to be 1.25 µg/mL at 24 hpf, 0.8 µg/mL at 48 hpf, and 0.7 µg/mL at 72 hpf, demonstrating bonducellin's strong bioactivity even at lower concentrations.

Gene expression analysis in zebrafish embryos

The gene expression analysis was performed using RT-PCR to evaluate the effect of bonducellin on *MMP9* expression in zebrafish embryos at the mRNA level. RNA was isolated from two groups, control and bonducellin-treated (0.8 µg/mL) at 24 and 48 hpf. The isolated RNA was converted into cDNA and used for gene expression analysis. Gel electrophoresis confirmed the successful amplification of *MMP9* and *β-Actin*, and quantitative analysis using ImageJ software revealed a 0.05-fold downregulation of *MMP9* expression at 24 hpf compared to the control. However, *MMP9* expression was significantly upregulated (2.4-fold) at 48 hpf. The housekeeping gene *β-Actin* was used for normalization, ensuring accurate quantification of expression levels (Figure 15).

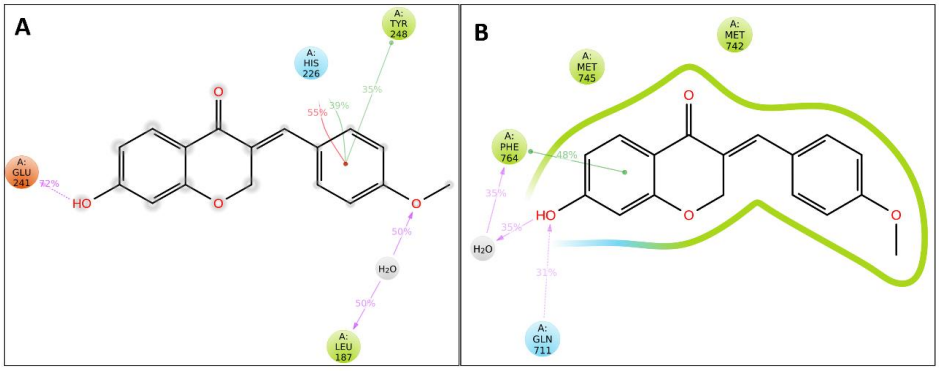

Figure 11 2D interaction diagram showing interaction formed between ligands and proteins. (A) Bonducellin-MMP9 complex. (B) Bonducellin-AR complex.

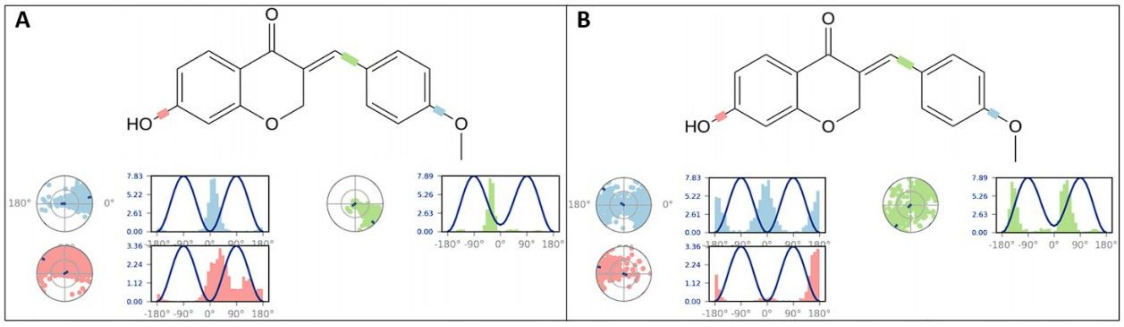

Figure 12 Ligand torsion profile between ligands and proteins. (A) Bonducellin-MMP9 complex. (B) Bonducellin-AR complex.

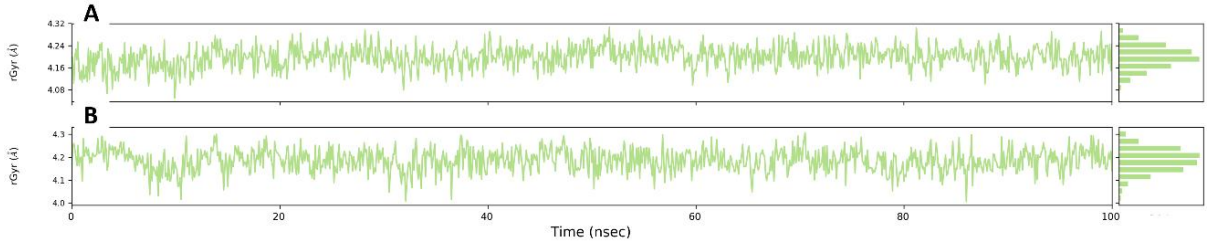

Figure 13 The radius of gyration plots during a 100 ns molecular simulation. (A) Bonducellin-MMP9 complex. (B) Bonducellin-AR complex.

Traditional Medicine Research 2025;10(11):65. https://doi.org/10.53388/TMR20241216001

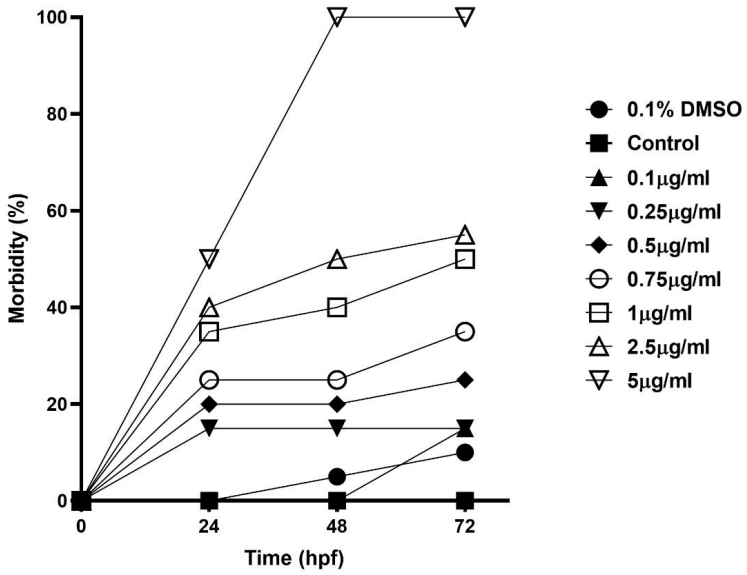

Figure 14 The morbidity of zebrafish embryos treated with bonducellin at various concentrations. 0.1% DMSO served as vehicle control.

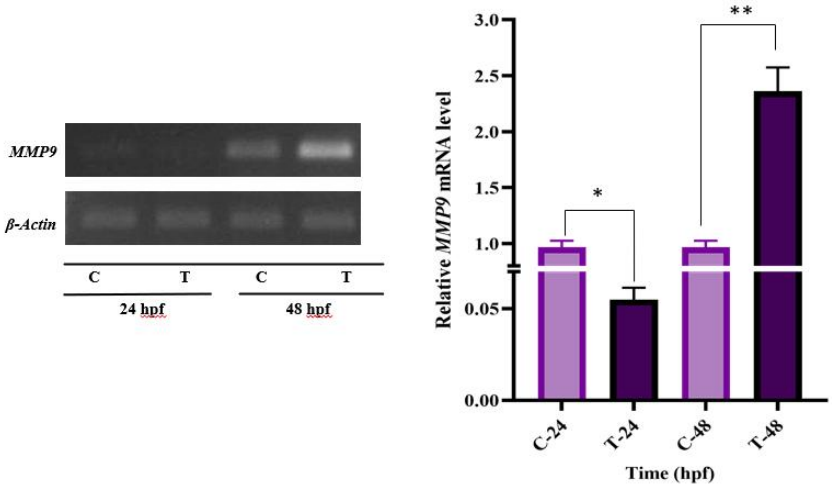

Figure 15 The relative expression of *MMP9 in* zebrafish embryos treated with 0.8 μg/mL bonducellin. The values are expressed as mean ± SD of three replicates of the experiments, n = 10, and the asterisks indicate statistically significant differences at $^{*}P < 0.05$, $^{**}P < 0.01$ between the bonducellin-treated (T) and control (C) groups. *MMP9*, Matrix Metalloproteinase-9.

Discussion

PCOS has become one of the most common metabolic and endocrine ailments in women of reproductive age, necessitating immediate attention to curb its alarming increase in prevalence. Although there are several herbal medications recommended for the management of PCOS, the seed kernels of the medicinal plant, *Caesalpinia bonducella,* have recently been in the limelight due to their anti-androgenic and anti-estrogenic properties and also due to their ability to balance the hormones and dysregulated lipid profiles associated with PCOS [66]. The therapeutic potential of *C. bonducella* seeds is attributed to the bioactive phytochemicals like flavonoids, sterols, cassane, and furanoditerpenes [17], where bonducellin is one of the major bioactive homoisoflavonoid effective against various disorders associated with PCOS. Owing to its importance, we aimed to identify the molecular mechanism underlying the therapeutic properties of bonducellin through the network pharmacology approach.

In this study, 100 genes that are possible targets for bonducellin were identified using SWISS target prediction. Of these genes, 76 genes that are involved in the pathogenesis of PCOS and its associated risks such as diabetes, insulin resistance, obesity, ovarian cancer, metabolic syndrome, endometrial cancer, and inflammation were filtered by Venn analysis, which when subjected to GO enrichment and KEGG pathway enrichment analysis showed that they are involved in 15 important pathways, including ovarian steroidogenesis, GnRH signaling, and insulin resistance. Sixteen proteins (MMP9, AR, KDR, PRKACA, KIT, CYP19A1, HSD11B1, ESR1, STAT3, ESR2, PRKCA, ROCK1, BRAF, HSD17B2, PIK3R1, RAF1) that showed higher PPI were chosen for docking against bonducellin to identify the latter's potential targets and mode of action. Here, we further discuss the ovarian steroidogenesis pathway, which is essential for regulating the female reproductive system, influencing processes such as ovulation, menstruation, and pregnancy. Understanding how bonducellin modulates this pathway is crucial for addressing reproductive health issues and developing therapeutic interventions for conditions such as PCOS.

Two proteins, MMP9 and AR, that showed a higher binding affinity with bonducellin were subjected to MD simulations to evaluate their stability in a solvated environment. MMP9, a matrix metalloproteinase, plays a crucial role in extracellular matrix remodeling. In normal women, the protease activity of MMP9 within the extracellular matrix is regulated by the tissue inhibitors of MMPs (TIMPs) [67]. However, in PCOS women, an increased expression of MMP9 and a deregulated MMP9:TIMP1 ratio were observed in the ovaries, which may result in excessive remodeling of ovarian follicles

and walls, thus impairing the ovarian cycle [68]. A disruption in the balance between MMPs and TIMPs has been associated with the pathophysiology of several diseases. It is believed that excessive androgen secretion in PCOS women can alter the balance of MMPs and TIMPs in the ovaries, resulting in the progression of fibrosis and follicular atresia [69]. Administration of an additional inhibitor can reduce the activity of MMP9 in PCOS women. In this study, strong binding of bonducellin (−11.25 kcal/mol) to MMP9 was predicted by docking, where MMP9 interacts with 29 key proteins related to PCOS, which shows that it may possess an impending role in balancing the MMP9: TIMP1 ratio in PCOS women and thereby preventing ovarian dysfunction.

The ligand-dependent nuclear transcription factor, AR, plays a crucial role in mediating androgen biosynthesis, including testosterone and dihydrotestosterone. ARs are involved in various biological functions, such as system maintenance and development [70]. Increased GnRH levels lead to a surge in LH in women, which, in turn, promotes elevated androgen production. Elevated androgen levels are a hallmark of PCOS globally. Excess androgens trigger a cascade of cellular events via the androgen receptors [71]. In this study, molecular docking has predicted a strong binding affinity (−9.4 kcal/mol) between bonducellin and ARs, demonstrating an interaction with 15 key proteins associated with PCOS. This suggests that bonducellin has the potential to inhibit AR activity, thereby mitigating manifestations of excess androgens, such as hyperandrogenism and hirsutism in women with PCOS.

While excess androgen is the hallmark of PCOS, induction of ovulation in PCOS women for treating infertility is done by inhibiting aromatase using letrozole and other commercial aromatase inhibitors. The aromatase enzyme is coded by the *CYP19A1* gene, which plays a crucial role in the biosynthesis of estrogen from androstenedione [72]. Reduction in the estrogen level leads to increased FSH hormone, creating a feedback loop. As the level of FSH rises, the aromatase level increases [73]. Hence, aromatase inhibitors help in the balanced maintenance of estrogen. As commercial inhibitors show adverse side effects, there is a constant search for novel inhibitors from natural resources. A high affinity of bonducellin (−8.29 kcal/mol) to aromatase unveils its potential to inhibit the enzyme and thereby assist in treating infertility. Bonducellin is not only a strong target for *CYP19A1* but also *HSD11B1* (hydroxysteroid 11-beta dehydrogenase 1) and *HSD17B2* (17-beta-hydroxysteroid dehydrogenase), with binding affinities of −7.98 kcal/mol and −6.62 kcal/mol, respectively. These enzymes are involved in the conversion of androstenedione to testosterone in the ovarian steroidogenesis pathway and thus can help regulate androgen levels. Thus, bonducellin demonstrates its anti-androgenic and anti-estrogenic properties.

Furthermore, the estrogen receptors (ERα and ERβ) are another high-affinity target for bonducellin with −7.59 kcal/mol and −7.26 kcal/mol, respectively, found in the network pharmacological studies. In humans, two isoforms of estrogen receptors, ERα and ERβ, have been reported [74, 75]. ERs, the transcription factors belonging to the nuclear receptor family, are found in the nucleus, cytoplasm, and mitochondria and help in estrogen-mediated signaling and transcription of downstream genes [76]. PCOS is the manifestation of excess androgen and altered estrogen, which in turn disrupts the HPA axis, resulting in increased LH secretion [77]. Regulating estrogen levels is the first-line treatment for PCOS-caused infertility in women. Many selective estrogen receptor modulators, like clomiphene citrate (CC), are recommended for inducing ovulation by increasing the secretion of LH and FSH from the hypothalamus. CC functions like an agonist at reduced endogenous estrogen levels or largely as an antagonist of ER [78, 79]. CC is believed to affect the ER in the hypothalamus, wherein it improves the secretion of LH frequency to promote ovulation [80]. Bonducellin, the compound under study, with a high binding affinity to *ESR1* and *ESR2*, could be a promising novel selective estrogen receptor modulator that can modulate the effect of estrogen receptors.

STAT3, which is a transcription factor, plays a crucial role in various cellular processes, including cell proliferation and cell differentiation. It is also involved in ovarian steroidogenesis, contributing to the upregulation of *LHCGR, CYP17a,* and *p450C17a* and downregulating the expression levels of *FSHR, CYP19*, and aromatase, thereby leading to polycystic ovarian morphology [81]. The affinity of bonducellin is −7.32 kcal/mol towards STAT3 protein, which showed a higher level of protein interaction amongst 43 key targets of PCOS, which could potentially help in alleviating PCOS. Bonducellin could mechanistically bind to the downstream targets of STAT3, i.e., *LHCGR*, *FSHR*, *CYP17a*, and *CYP19*, and alter their expression, benefiting follicular development.

To evaluate the safety of bonducellin, zebrafish embryo toxicity assays were performed for 24, 48, and 72 h post-fertilization (hpf). The LC_{50} values of bonducellin were determined as 1.25 μg/mL at 24 hpf, 0.8 μg/mL at 48 hpf, and 0.7 μg/mL at 72 hpf. These values suggest a dose-dependent toxicity profile, which should be considered for future pharmacological studies. Gene expression analysis revealed a significant downregulation of *MMP9* (0.05-fold) at 24 hpf, followed by a notable upregulation (2.4-fold) at 48 hpf. This biphasic expression pattern suggests a feedback regulatory mechanism, as *MMP9* is essential for extracellular matrix remodeling and embryonic development. This finding stands as a preliminary study to show that bonducellin modulates the expression of the target genes.

Conclusion

PCOS is a multifactorial and multisystem disorder associated with various symptomatic complications, including hormonal imbalances, dysregulated cholesterol levels, and impaired glucose metabolism, all of which require immediate attention and care. Patients with PCOS often require multiple medications to address underlying symptoms, as there is currently no single drug that can effectively target all manifestations of the condition. The use of *Caesalpinia bonducella* seeds by PCOS patients has been reported to reduce cyst formation, regulate hormone levels, reduce blood sugar, induce ovulation, and improve menstrual cycles. In the present study, we investigated the potential molecular mechanism underlying the efficacy of bonducellin, a homoisoflavonoid from *C. bonducella*, on PCOS and its symptomatic disorders through network pharmacology. The findings identified that bonducellin could target the key proteins and receptors associated with PCOS and possibly alter their expression or their downstream targets. Given its promising pharmacological properties, bonducellin could serve as a natural alternative for PCOS management. Albeit the toxicity studies are performed in zebrafish embryos, the profound effects of the treatment require further *in vivo* investigations and clinical trials. Understanding its precise molecular interactions and long-term effects is crucial in advancing bonducellin as a novel therapeutic strategy for PCOS.

References

1. Ke Y, Hu J, Zhu Y, Wang Y, Chen S, Liu S. Correlation between circulating adropin levels and patients with PCOS: An updated systematic review and meta-analysis. *Reprod Sci.* 2022;29(12):3295–3310. Available at: http://doi.org/10.1007/s43032-022-00841-1
2. Duică F, Dănilă CA, Boboc AE, et al. Impact of increased oxidative stress on cardiovascular diseases in women with polycystic ovary syndrome. *Front Endocrinol (Lausanne).* 2021;12:614679. Available at: http://doi.org/10.3389/fendo.2021.614679
3. Koohnavard F, Ahmadi K, Eftekhar E, Edalatmanesh MA. Computational screening of FDA-approved drugs to identify potential aromatase receptor inhibitors for polycystic ovary syndrome. *J Biomol Struct Dyn.* 2023;41(24):15507–15519. Available at: http://doi.org/10.1080/07391102.2023.2190411
4. Moka MK, Ankul SS, Sumithra M. Computational investigation of four isoquinoline alkaloids against polycystic ovarian

syndrome. *J Biomol Struct Dyn.* 2024;42(2):734–746. Available at: http://doi.org/10.1080/07391102.2023.2222828
5. Azziz R, Carmina E, Chen Z, et al. Polycystic ovary syndrome. *Nat Rev Dis Primers.* 2016;22:16057. Available at: http://doi.org/10.1038/nrdp.2016.57
6. Helvaci N, Yildiz BO. Current and emerging drug treatment strategies for polycystic ovary syndrome. *Expert Opin Pharmacother.* 2023;24(1):105–120. Available at: http://doi.org/10.1080/14656566.2022.2108702
7. Zeng LH, Rana S, Hussain L, et al. Polycystic Ovary Syndrome: A disorder of reproductive age, its pathogenesis, and a discussion on the emerging role of herbal remedies. *Front Pharmacol.* 2022;13:874914. Available at: http://doi.org/10.3389/fphar.2022.874914
8. Moini Jazani A, Nasimi Doost Azgomi H, Nasimi Doost Azgomi A, Nasimi Doost Azgomi R. A comprehensive review of clinical studies with herbal medicine on polycystic ovary syndrome (PCOS). *Daru.* 2019;27(2):863–877. Available at: http://doi.org/10.1007/s40199-019-00312-0
9. Qin B, Nagasaki M, Ren M, Bajotto G, Oshida Y, Sato Y. Cinnamon extract (traditional herb) potentiates in vivo insulin-regulated glucose utilization via enhancing insulin signaling in rats. *Diabetes Res Clin Pract.* 2003;62(3):139–148. Available at: http://doi.org/10.1016/S0168-8227(03)00173-6
10. Yang H, Kim HJ, Pyun BJ, Lee HW. Licorice ethanol extract improves symptoms of polycytic ovary syndrome in Letrozole-induced female rats. *Integr Med Res.* 2018;7(3):264–270. Available at: http://doi.org/10.1016/j.imr.2018.05.003
11. Nowak DA, Snyder DC, Brown AJ, Demark-Wahnefried W. The effect of flaxseed supplementation on hormonal levels associated with polycystic ovarian syndrome: A case study. *Curr Top Nutraceutical Res.* 2007;5(4):177–181. Available at: https://www.ncbi.nlm.nih.gov/pubmed/19789727
12. Nassiri-Asl M, Zamansoltani F, Abbasi E, Daneshi MM, Zangivand AA. Effects of Urtica dioica extract on lipid profile in hypercholesterolemic rats. *Zhong Xi Yi Jie He Xue Bao.* 2009;7(5):428–433. Available at: https://pubmed.ncbi.nlm.nih.gov/19435556/
13. Moini Jazani A, Hamdi K, Tansaz M, et al. Herbal medicine for oligomenorrhea and amenorrhea: a systematic review of ancient and conventional medicine. *Biomed Res Int.* 2018;2018:3052768. Available at: http://doi.org/10.1155/2018/3052768
14. Swaroop A, Jaipuriar AS, Gupta SK, et al. Efficacy of a novel fenugreek seed extract (Trigonella foenum-graecum, FurocystTM) in Polycystic Ovary Syndrome (PCOS). *Int J Med Sci.* 2015;12(10):825–831. Available at: http://doi.org/10.7150/ijms.13024
15. Kuppachi H, Kandasamy V, Balasundaram U. In-silico screening of potential anti-androgenic and anti-estrogenic phytocompounds from Saraca asoca for polycystic ovary syndrome treatment. *J Appl Pharm Sci.* 2024;14(2):261–272. Available at: http://doi.org/10.7324/JAPS.2024.146675
16. Himaja K, Veerapandiyan K, Usha B. Aromatase inhibitors identified from Saraca asoca to treat infertility in women with polycystic ovary syndrome via in silico and in vivo studies. *J Biomol Struct Dyn.* 2024:1–16. Available at: http://doi.org/10.1080/07391102.2024.2310793
17. Kandasamy V, Balasundaram U. Caesalpinia bonduc (L.) Roxb. as a promising source of pharmacological compounds to treat Polycystic Ovary Syndrome (PCOS): A review. *J Ethnopharmacol.* 2021:279:114375. Available at: http://doi.org/10.1016/j.jep.2021.114375
18. Meera B, Muralidharan P, Hari R. Antioxidant potential of Caesalpinia bonducella seeds in the management of polycystic ovary syndrome (PCOS) using mifepristone induced rats model. *J Herbs Spices Med Plants.* 2020;27(2):123–134. Available at: http://doi.org/10.1080/10496475.2020.1795041
19. Ojha MD, Yadav A, Hariprasad P. Analyzing the potential of selected plant extracts and their structurally diverse secondary metabolites for α-glucosidase inhibitory activity: in vitro and in silico approach. *J Biomol Struct Dyn.* 2023;41(19):9523–9538. Available at: http://doi.org/10.1080/07391102.2022.2142847
20. Karthikeyan M, Akshatha P, Mohideen HS, Usha B. Caesalpinia bonducella seeds extracts are non-toxic to the gut bacteria Lactobacillus rhamnosus, as substantiated by in vitro and in silico studies. *J Pure Appl Microbiol.* 2024;18(3):2070–2084. Available at: http://doi.org/10.22207/JPAM.18.3.57
21. Lakshmi JN, Babu AN, Kiran SSM, et al. Herbs as a source for the treatment of polycystic ovarian syndrome: a systematic review. *BioTech (Basel).* 2023;12(1):4. Available at: http://doi.org/10.3390/biotech12010004
22. Meera Murugesan B, Muralidharan P, Hari R. Effect of ethanolic seed extract of Caesalpinia bonducella on hormones in mifepristone induced PCOS rats. *J Appl Pharm Sci.* 2020;10(2):72–76. Available at: http://doi.org/10.7324/JAPS.2020.102012
23. Castelli MV, López SN. Homoisoflavonoids: occurrence, biosynthesis, and biological activity. *Stud Nat Prod Chem.* 2017;54:315–354. Available at: http://doi.org/10.1016/B978-0-444-63929-5.00009-7
24. McPherson DD, Cordell GA, Soejarto DD, Pezzuto JM, Fong HHS. Peltogynoids and homoisoflavonoids from Caesalpinia pulcherrima. *Phytochemistry.* 1983;22(12):2835–2838. Available at: http://doi.org/10.1016/S0031-9422(00)97708-2
25. Li DM, Ma L, Liu GM, Hu LH. Cassane diterpene-lactones from the seed of Caesalpinia minax Hance. *Chem Biodivers.* 2006;3(11):1260–1265. Available at: http://doi.org/10.1002/cbdv.200690128
26. Chen P, Yang JS. Flavonol galactoside caffeiate ester and homoisoflavones from Caesalpinia millettii HOOK. *Chem Pharm Bull (Tokyo).* 2007;55(4):655–657. Available at: http://doi.org/10.1248/cpb.55.655
27. Rao YK, Fang SH, Tzeng YM. Anti-inflammatory activities of flavonoids isolated from Caesalpinia pulcherrima. *J Ethnopharmacol.* 2005;100(3):249–253. Available at: http://doi.org/10.1016/j.jep.2005.02.039
28. Roy SK, Kumari N, Gupta S, Pahwa S, Nandanwar H, Jachak SM. 7-Hydroxy-(E)-3-phenylmethylene-chroman-4-one analogues as efflux pump inhibitors against Mycobacterium smegmatis mc^2 155. *Eur J Med Chem.* 2013;66:499–507. Available at: http://doi.org/10.1016/j.ejmech.2013.06.024
29. Dong TH, Ning AYW, Tang YQ. Network pharmacology-integrated molecular docking analysis of phytocompounds of Caesalpinia pulcherrima (peacock flower) as potential anti-metastatic agents. *J Biomol Struct Dyn.* 2024;42(4):1778–1794. Available at: http://doi.org/10.1080/07391102.2023.2202273
30. Kandasamy V, Sathish S, Madhavan T, Balasundaram U. In-silico screening of phytochemical compounds in Caesalpinia bonducella L. seeds against the gene targets of ovarian steroidogenesis pathway. *J Microbiol Biotechnol Food Sci.* 2023;13(2):e6124. Available at: http://doi.org/10.55251/jmbfs.6124
31. Fotis C, Antoranz A, Hatziavramidis D, Sakellaropoulos T, Alexopoulos LG. Network-based technologies for early drug discovery. *Drug Discov Today.* 2018;23(3):626–635. Available at: http://doi.org/10.1016/j.drudis.2017.12.001
32. Sabarathinam S, Ganamurali N. Chalcones reloaded: an integration of network pharmacology and molecular docking for type 2 diabetes therapy. *J Biomol Struct Dyn.*

2024;42(18):9505–9517. Available at: http://doi.org/10.1080/07391102.2023.2252085
33. Ji W, Wang TT, Xu YW, An R, Liang K, Wang XH. Identifying the active compounds and mechanism of action of Banxia Xiexin decoction for treating ethanol-induced chronic gastritis using network pharmacology combined with UPLC-LTQ-Orbitrap MS. *Comput Biol Chem.* 2021;93:107535. Available at: http://doi.org/10.1016/j.compbiolchem.2021.107535
34. Li J, Jia NN, Cui MY, Li YQ, Jiang DY, Chu XQ. Chinese herb couple against diabetes: integrating network pharmacology and mechanism study. *J Biomol Struct Dyn.* 2024:1–17. Available at: http://doi.org/10.1080/07391102.2024.2314263
35. Li S, Zhang B. Traditional Chinese medicine network pharmacology: theory, methodology and application. *Chin J Nat Med.* 2013;11(2):110–120. Available at: http://doi.org/10.1016/S1875-5364(13)60037-0
36. Nandi A, Nigar T, Das A, Dey YN. Network pharmacology analysis of Plumbago zeylanica to identify the therapeutic targets and molecular mechanisms involved in ameliorating hemorrhoids. *J Biomol Struct Dyn.* 2025;43(1):161–175. Available at: http://doi.org/10.1080/07391102.2023.2280681
37. Chahardehi AM, Arsad H, Lim V. Zebrafish as a successful animal model for screening toxicity of medicinal plants. *Plants (Basel)*. 2020;9(10):1345. Available at: http://doi.org/10.3390/plants9101345
38. Daina A, Michielin O, Zoete V. SwissADME: a free web tool to evaluate pharmacokinetics, drug-likeness and medicinal chemistry friendliness of small molecules. *Sci Rep.* 2017;7:42717. Available at: http://doi.org/10.1038/srep42717
39. Kim S, Chen J, Cheng TJ, et al. PubChem 2019 update: improved access to chemical data. *Nucleic Acids Res.* 2019;47(D1):D1102–D1109. Available at: http://doi.org/10.1093/nar/gky1033
40. Piñero J, Bravo À, Queralt-Rosinach N, et al. DisGeNET: a comprehensive platform integrating information on human disease-associated genes and variants. *Nucleic Acids Res.* 2017;45(D1):D833–D839. Available at: http://doi.org/10.1093/nar/gkw943
41. Szklarczyk D, Morris JH, Cook H, et al. The STRING database in 2017: quality-controlled protein–protein association networks, made broadly accessible. *Nucleic Acids Res.* 2017;45(D1):D362–D368. Available at: http://doi.org/10.1093/nar/gkw937
42. Shannon P, Markiel A, Ozier O, et al. Cytoscape: A Software Environment for Integrated Models of Biomolecular Interaction Networks. *Genome Res.* 2003;13(11):2498–2504. Available at: http://doi.org/10.1101/gr.1239303
43. Chin CH, Chen SH, Wu HH, Ho CW, Ko MT, Lin CY. cytoHubba: identifying hub objects and sub-networks from complex interactome. *BMC Syst Biol.* 2014;8 Suppl 4(Suppl 4):S11. Available at: http://doi.org/10.1186/1752-0509-8-S4-S11
44. Nuti E, Cuffaro D, Bernardini E, et al. Development of thioaryl-based matrix metalloproteinase-12 inhibitors with alternative zinc-binding groups: Synthesis, potentiometric, NMR, and crystallographic studies. *J Med Chem.* 2018;61(10):4421–4435. Available at: http://doi.org/10.1021/acs.jmedchem.8b00096
45. Nadal M, Prekovic S, Gallastegui N, et al. Structure of the homodimeric androgen receptor ligand-binding domain. *Nat Commun.* 2017;8:14388. Available at: http://doi.org/10.1038/ncomms14388
46. Okamoto K, Ikemori-Kawada M, Jestel A, et al. Distinct binding mode of multikinase inhibitor lenvatinib revealed by biochemical characterization. *ACS Med Chem Lett.* 2014;6(1):89–94. Available at: http://doi.org/10.1021/ml500394m
47. Breitenlechner C, Gassel M, Hidaka H, et al. Protein kinase A in complex with Rho-kinase inhibitors Y-27632, Fasudil, and H-1152P: structural basis of selectivity. *Structure.* 2003;11(12):1595–1607. Available at: http://doi.org/10.1016/j.str.2003.11.002
48. Tian W, Yan P, Xu N, et al. The HRP3 PWWP domain recognizes the minor groove of double-stranded DNA and recruits HRP3 to chromatin. *Nucleic Acids Res.* 2019;47(10):5436–5448. Available at: http://doi.org/10.1093/nar/gkz294
49. Ghosh D, Egbuta C, Lo J. Testosterone complex and non-steroidal ligands of human aromatase. *J Steroid Biochem Mol Biol.* 2018;181:11–19. Available at: http://doi.org/10.1016/j.jsbmb.2018.02.009
50. Goldberg FW, Leach AG, Scott JS, et al. Free-Wilson and structural approaches to co-optimizing human and rodent isoform potency for 11β-hydroxysteroid dehydrogenase type 1 (11β-HSD1) inhibitors. *J Med Chem.* 2012;55(23):10652–10661. Available at: http://doi.org/10.1021/jm3013163
51. Norman BH, Richardson TI, Dodge JA, et al. Benzopyrans as selective estrogen receptor beta agonists (SERBAs). Part 4: functionalization of the benzopyran A-ring. *Bioorg Med Chem Lett.* 2007;17(18):5082–5085. Available at: http://doi.org/10.1016/j.bmcl.2007.07.009
52. Bai L, Zhou H, Xu R, et al. A potent and selective small-molecule degrader of STAT3 achieves complete tumor regression in vivo. *Cancer Cell.* 2019;36(5):498–511.e17. Available at: http://doi.org/10.1016/j.ccell.2019.10.002
53. Möcklinghoff S, Rose R, Carraz M, Visser A, Ottmann C, Brunsveld L. Synthesis and crystal structure of a phosphorylated estrogen receptor ligand binding domain. *Chembiochem.* 2010;11(16):2251–2254. Available at: http://doi.org/10.1002/cbic.201000532
54. Wagner J, von Matt P, Sedrani R, et al. Discovery of 3-(1H-indol-3-yl)-4-[2-(4-methylpiperazin-1-yl)quinazolin-4-yl] pyrrole-2,5-dione (AEB071), a potent and selective inhibitor of protein kinase C isotypes. *J Med Chem.* 2009;52(20):6193–6196. Available at: http://doi.org/10.1021/jm901108b
55. Li R, Martin MP, Liu Y, et al. Fragment-based and structure-guided discovery and optimization of Rho kinase inhibitors. *J Med Chem.* 2012;55(5):2474–2478. Available at: http://doi.org/10.1021/jm201289r
56. Stewart NK, Toth M, Stasyuk A, Vakulenko SB, Smith CA. In Crystallo Time-Resolved Interaction of the Clostridioides difficile CDD-1 enzyme with Avibactam Provides New Insights into the Catalytic Mechanism of Class D β-lactamases. *ACS Infect Dis.* 2021;7(6):1765–1776. Available at: http://doi.org/10.1021/acsinfecdis.1c00094
57. Li T, Song X, Stephen P, Yin H, Lin SX. New insights into the substrate inhibition of human 17β-hydroxysteroid dehydrogenase type 1. *J Steroid Biochem Mol Biol.* 2023;228:106246. Available at: http://doi.org/10.1016/j.jsbmb.2023.106246
58. Hart JR, Liu X, Pan C, et al. Nanobodies and chemical cross-links advance the structural and functional analysis of PI3Kα. *Proc Natl Acad Sci U S A.* 2022;119(38):e2210769119. Available at: http://doi.org/10.1073/pnas.2210769119
59. García-Alonso S, Mesa P, Ovejero LP, et al. Structure of the RAF1-HSP90-CDC37 complex reveals the basis of RAF1 regulation. *Mol Cell.* 2022;82(18):3438–3452.e8. Available at: http://doi.org/10.1016/j.molcel.2022.08.012
60. Bowers KJ, Chow DE, Xu HF, et al. Scalable Algorithms for Molecular Dynamics Simulations on Commodity Clusters. In: *SC '06: Proceedings of the ACM/IEEE Conference on Supercomputing.* Tampa, FL: IEEE;2006. Available at: http://doi.org/10.1109/SC.2006.54
61. Sheoran S, Arora S, Basu T, et al. In silico analysis of diosmetin

as an effective chemopreventive agent against prostate cancer: molecular docking, validation, dynamic simulation and pharmacokinetic prediction-based studies. *J Biomol Struct Dyn.* 2024;42(17):9105–9117. Available at: http://doi.org/10.1080/07391102.2023.2250451

62. Ravi L, Kumar KA, Kumari GRS, et al. Stearyl palmitate a multi-target inhibitor against breast cancer: in-silico, in-vitro & in-vivo approach. *J Biomol Struct Dyn.* 2024;42(19):10057–10074. Available at: http://doi.org/10.1080/07391102.2023.2255271
63. Karthikeyan M, Baskar B, Kandasamy V, Balasundaram U. Glutathione elicits enhanced biosynthesis of bonducellin, a homoisoflavonoid, in Caesalpinia bonducella leaf callus. *Plant Cell Tiss Organ Cult.* 2023;155(1):57–65. Available at: http://doi.org/10.1007/s11240-023-02551-1
64. Litchfield JT Jr, Wilcoxon F. A simplified method of evaluating dose-effect experiments. *J Pharmacol Exp Ther.* 1949;96(2):99–113. Available at: http://doi.org/10.1016/S0022-3565(25)03549-9
65. Hazman M. Gel express: a novel frugal method quantifies gene relative expression in conventional RT-PCR. *Beni-Suef Univ J Basic Appl Sci.* 2022;11(1):11. Available at: http://doi.org/10.1186/s43088-022-00194-3
66. De Leo V, Musacchio MC, Cappelli V, Massaro MG, Morgante G, Petraglia F. Genetic, hormonal and metabolic aspects of PCOS: an update. *Reprod Biol Endocrinol.* 2016;14(1):38. Available at: http://doi.org/10.1186/s12958-016-0173-x
67. Shalev E, Goldman S, Ben-Shlomo I. The balance between MMP-9 and MMP-2 and their tissue inhibitor (TIMP)-1 in luteinized granulosa cells: comparison between women with PCOS and normal ovulatory women. *Mol Hum Reprod.* 2001;7(4):325–331. Available at: http://doi.org/10.1093/molehr/7.4.325
68. Dambala K, Vavilis D, Bili E, Goulis DG, Tarlatzis BC. Serum visfatin, vascular endothelial growth factor and matrix metalloproteinase-9 in women with polycystic ovary syndrome. *Gynecol Endocrinol.* 2017;33(7):529–533. Available at: http://doi.org/10.1080/09513590.2017.1296425
69. Zhou F, Shi LB, Zhang SY. Ovarian Fibrosis: A Phenomenon of Concern. *Chin Med J (Engl).* 2017;130(3):365–371. Available at: http://doi.org/10.4103/0366-6999.198931
70. Decourt C, Watanabe Y, Evans MC, et al. Deletion of Androgen Receptors From Kisspeptin Neurons Prevents PCOS Features in a Letrozole Mouse Model. *Endocrinology.* 2023;164(6):bqad077. Available at: http://doi.org/10.1210/endocr/bqad077
71. Gao XY, Liu Y, Lv Y, et al. Role of Androgen Receptor for Reconsidering the "True" Polycystic Ovarian Morphology in PCOS. *Sci Rep.* 2020;10(1):8993. Available at: http://doi.org/10.1038/s41598-020-65890-5
72. Davey RA, Grossmann M. Androgen receptor structure, function and biology: From bench to bedside. *Clin Biochem Rev.* 2016;37(1):3–15. Available at: https://www.ncbi.nlm.nih.gov/pubmed/27057074
73. Barbieri RL. The Endocrinology of the Menstrual Cycle. *Methods Mol Biol.* 2014;1154:145–169. Available at: http://doi.org/10.1007/978-1-4939-0659-8_7
74. Walter P, Green S, Greene G, et al. Cloning of the human estrogen receptor cDNA. *Proc Natl Acad Sci USA.* 1985;82(23):7889–7893. Available at: http://doi.org/10.1073/pnas.82.23.7889
75. Mosselman S, Polman J, Dijkema R. ERβ: Identification and characterization of a novel human estrogen receptor. *FEBS Lett.* 1996;392(1):49–53. Available at: http://doi.org/10.1016/0014-5793(96)00782-X
76. Xu XL, Deng SL, Lian ZX, Yu K. Estrogen Receptors in Polycystic Ovary Syndrome. *Cells.* 2021;10(2):459. Available at: http://doi.org/10.3390/cells10020459
77. Rosenfield RL, Ehrmann DA. The Pathogenesis of Polycystic Ovary Syndrome (PCOS): The Hypothesis of PCOS as Functional Ovarian Hyperandrogenism Revisited. *Endocr Rev.* 2016;37(5):467–520. Available at: http://doi.org/10.1210/er.2015-1104
78. Clark JH, Markaverich BM. The agonistic-antagonistic properties of clomiphene: a review. *Pharmacol Ther.* 1981;15(3):467–519. Available at: http://doi.org/10.1016/0163-7258(81)90055-3
79. Kettel LM, Roseff SJ, Berga SL, Mortola JF, Yen SSC. Hypothalamic-pituitary-ovarian response to clomiphene citrate in women with polycystic ovary syndrome. *Fertil Steril.* 1993;59(3):532–538. Available at: http://doi.org/10.1016/S0015-0282(16)55795-1
80. Sir T, Alba F, Devoto L, Rossmanith W. Clomiphene Citrate and LH Pulsatility in PCO Syndrome. *Horm Metab Res.* 1989;21(10):583. Available at: http://doi.org/10.1055/s-2007-1009293
81. Xiong AL, Yang ZD, Shen YC, Zhou J, Shen Q. Transcription Factor STAT3 as a Novel Molecular Target for Cancer Prevention. *Cancers (Basel).* 2014;6(2):926–957. Available at: http://doi.org/10.3390/cancers6020926